

STformer: A Noise-Aware Efficient Spatio-Temporal Transformer Architecture for Traffic Forecasting

Yanjun Qin

Beijing University of Posts and
Telecommunications
qinyanjun@bupt.edu.cn

Liang Zeng

Tsinghua University
zengl18@mails.tsinghua.edu.cn

Yuchen Fang*

Beijing University of Posts and
Telecommunications
fangyuchen@bupt.edu.cn

Fang Zhao†

Beijing University of Posts and
Telecommunications
zfsse@bupt.edu.cn

Haiyong Luo†

Institute of Computing Technology,
Chinese Academy of Sciences
yhuo@ict.ac.cn

Chenxing Wang

Beijing University of Posts and
Telecommunications
wangchenxing@bupt.edu.cn

ABSTRACT

Traffic forecasting plays an indispensable role in the intelligent transportation system, which makes daily travel more convenient and safer. However, the dynamic evolution of spatio-temporal correlations makes accurate traffic forecasting very difficult. Existing work mainly employs graph neural networks (GNNs) and deep time series models (e.g. recurrent neural networks) to capture complex spatio-temporal patterns in the dynamic traffic system. For the spatial patterns, it is difficult for GNNs to extract the global spatial information, *i.e.*, remote sensors information in road networks. Although we can use the self-attention to extract global spatial information as in the previous work, it is also accompanied by huge resource consumption. For the temporal patterns, traffic data have not only easy-to-recognize daily and weekly trends but also difficult-to-recognize short-term noise caused by accidents (e.g. car accidents and thunderstorms). Prior traffic models are difficult to distinguish intricate temporal patterns in time series and thus hard to get accurate temporal dependence. To address above issues, we propose a novel noise-aware efficient spatio-temporal Transformer architecture for accurate traffic forecasting, named STformer. STformer consists of two components, which are the noise-aware temporal self-attention (NATSA) and the graph-based sparse spatial self-attention (GBS3A). NATSA separates the high-frequency component and the low-frequency component from the time series to remove noise and capture stable temporal dependence by the learnable filter and the temporal self-attention, respectively. GBS3A replaces the full query in vanilla self-attention with the graph-based sparse query to decrease the time and memory usage. Experiments on four real-world traffic datasets show that STformer outperforms state-of-the-art baselines with lower computational cost.

CCS CONCEPTS

- Information systems → Spatial-temporal systems; • Computing methodologies → Neural networks.

KEYWORDS

traffic forecasting, spatio-temporal data, transformer, self-attention

*Equal contribution.

†Corresponding author.

1 INTRODUCTION

The traffic forecasting task aims to predict future traffic information (e.g. speed and volume) based on historical traffic conditions. Accurate forecasting assists traffic management departments in diverting traffic to avoid congestion and is beneficial for daily travel.

Traffic forecasting is very challenging because of its complex spatio-temporal dependencies. The early statistical methods, *e.g.*, ARIMA [30] and VAR [16], are difficult to capture the non-linear temporal dependence in real-world traffic time series. The standard machine learning methods, *e.g.*, SVR [31] and KNN [25], can capture the non-linear temporal dependence and the spatial dependence. However, they mostly rely on the hand-craft features, resulting in weak generalization performance.

With the success of deep learning [8] used in computer vision [7], natural language processing [15], and speech recognition [9] in recent years. [12, 26, 32] use deep time series models such as Temporal Convolution Networks (TCNs), Self-Attention Networks (SANs), and Recurrent Neural Networks (RNNs) to extract non-linear temporal dependence of each sensor individually for traffic forecasting. However, these methods ignore the impact of complex spatial dependence on traffic data. Subsequently, [14, 19, 33, 34] combine deep models that can capture spatial dependence (*e.g.* graph neural networks (GNNs) and SANs) with deep time series models mentioned above and achieve significant results.

Nevertheless, prior methods neglect some issues in the spatial and temporal dimensions. For the spatial dimension, the global spatial receptive field brings more useful information than the local does. However, whether we use GNNs or SANs to extract the global spatial information, they take a lot of time and memory to train. Concretely, most GNN-based models receive information of neighboring nodes, and they capture distant information by stacking GNN layers. But the more GNN layers are stacked, the more difficult to optimize it. Moreover, the SAN-based models have a quadratic issue, *i.e.*, the time complexity and memory usage is $O(N^2)$ on a graph with N vertexes. Although GMAN [35] proposes an algorithm for grouping nodes to optimize SAN, the time complexity in GMAN is still exponential. For the temporal dimension, as shown in Figure 1a and 1c, traffic time series contains not only stable daily periodic patterns but also short-term fluctuations caused by accidents. Moreover, the fluctuations in the black circle in Figure 1c

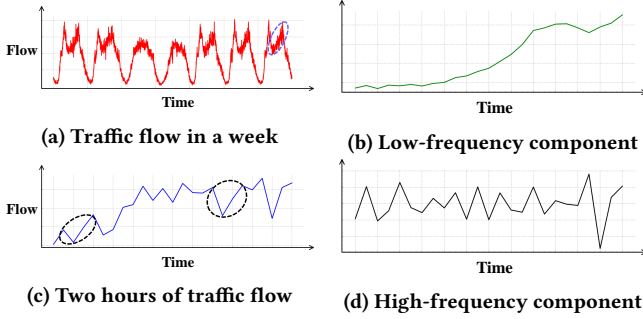


Figure 1: (a): The traffic flow recorded by a sensor in a week. (c): The enlarged view of the two hours traffic flow in the blue circle in (a). (b): The low-frequency component of (c) after discrete wavelet transform (DWT). (d): The high-frequency component of (c) after DWT.

are deviate from the long-term trend of low-frequency component in Figure 1b, thus these fluctuations cannot bring positive effects for traffic forecasting and are noise for the future. We consider the existing of noise will decrease prediction accuracy. However, prior traffic forecasting models ignore to remove noise in time series.

To capture the global spatial dependence efficiently and remove the noise in the traffic time series, we propose a novel noise-aware efficient Transformer architecture, named STformer. Inspired by the state-of-the-art self-attention optimization method ProbSparse Self-Attention (PBSA) [36], we design a Graph-Based Sparse Spatial Self-Attention (GBS3A) to extract global spatial information efficiently. Concretely, GBS3A utilizes the sparse query to replace the full query in the vanilla self-attention, and the sparse query consists of sensors with max flow from other sensors on the road network based graph. On the other hand, different from directly using discrete wavelet transform (DWT) [22] to remove the noise in time series. We propose a Noise-Aware Temporal Self-Attention (NATSA) in STformer, which uses the learnable filter and the self-attention for the high and low frequency component of time series after DWT to determine whether the high-frequency component are noise and extract the stable temporal dependence from the low-frequency component.

The main contributions of this paper are summarized as:

- We propose GBS3A to efficiently extract global spatial information, which significantly reduces memory and time consumption compared with vanilla self-attention.
- We propose NATSA to identify noise from high-frequency component and extract stable temporal information from low-frequency component.
- We propose STformer, which is a noise-aware efficient Transformer architecture, and we evaluate it on four real-world traffic datasets. Experimental results demonstrate that STformer outperforms all baselines.

2 RELATED WORK

Traffic Forecasting. Early researches [16, 30] use the traditional statistical methods which are based on linear assumptions to predict traffic. Later, [25, 31] apply machine learning in traffic forecasting

(e.g. SVR and KNN). The limitation of machine learning models is they require hand-craft features and are hard to generalize. With the success of deep learning in many fields, [28, 29] apply RNNs in traffic forecasting tasks. However, because of they neglect the spatial correlations in road networks and the noise in time series, the performance of them is not significantly improved. In spatial dimension, researchers utilize GNNs to extract the spatial information from non-Euclidean road networks, such as DCRNN and STGCN [14, 34]. Subsequent work considers building a dynamic graph for traffic forecasting. Graph WaveNet [33] uses learnable parameters to learn posterior node vectors to calculate the adjacency matrix through a data-driven manner. STGNN [27] uses dot products for hidden states in GRU to calculate the dynamic adjacency matrix. STGCN and STFGNN [18, 23] design a learnable parameter matrix to multiply the adjacency matrix and adjust the weights of the adjacency matrix through backpropagation. GMAN and ST-GRAT [19, 35] apply SAN in spatial dimension to capture the global spatial dependence, which avoid over-smoothing of stacking GNN. However, the SAN-based methods are inefficient in large-scale traffic data.

Attention Model. Attention firstly appear in the translation task, [1] propose the additive attention to improve the word alignment of the encoder-decoder architecture. Then, the widely used dot-product attention proposed by [17]. The additive attention and dot-product attention are mostly used in RNN-based encoder-decoder frameworks. Subsequently, [26] propose the Transformer, which is a pure attention model, and the Transformer achieves brilliant success in NLP [15] and CV [7]. However, the quadratic issue of self-attention hinders the application of Transformer to large-scale datasets. The Image Transformer [20] and Sparse Transformer [5] restrict the receptive field of the self-attention to a fixed local neighbor. Reformer and Routing Transformer [11, 21] use the dynamic pattern to replace the static fixed pattern. Set Transformer [13] proposes a novel global memory which access the entire sequence and Longformer [3] combines the global memory with a fixed pattern. Finally, Informer [36] takes query-key pairs in self-attention that away from the uniform distribution as dominate pairs to get the global memory. Besides, the proposed ProbSparse Self-Attention in Informer is the state-of-the-art method of efficient self-attention.

3 PRELIMINARY

Problem Definition. We use the three-dimensional tensor $X \in \mathbb{R}^{T \times N \times F}$ for traffic forecasting, which records F features by N sensors of T timeslices. We set $F = 1$ to represent traffic volume. The data at time t is $X_t \in \mathbb{R}^{N \times F}$, and $X^i \in \mathbb{R}^{T \times F}$ denotes the i -th sensor features of all timesteps. To represent the topological connection of road network, the graph of road network is defined as $\mathcal{G} = (\mathcal{V}, \mathcal{E}, \mathcal{A})$, where $\mathcal{V} \in \mathbb{R}^N$ denotes a finite node set, i.e., we record N sensors' data on the road network. \mathcal{E} is the edge set, and $\mathcal{A} \in \mathbb{R}^{N \times N}$ denotes the adjacency matrix based on \mathcal{E} , e.g., if sensors i and sensor j are adjacency on the road network, there will be an edge between them and $\mathcal{A}_{i,j} = 1$. The aim of traffic forecasting is learning a function \mathcal{F} , which learn from historical data $X = \{X_1, X_2, \dots, X_{T_h}\} \in \mathbb{R}^{T_h \times N \times F}$ to predict next T_p traffic data

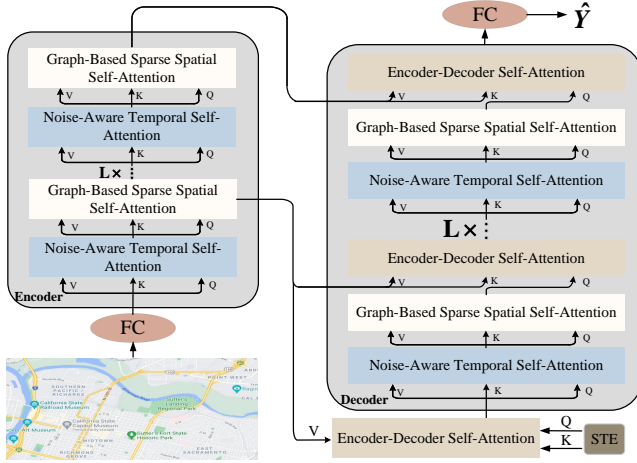


Figure 2: The proposed STformer for traffic forecasting, where FC and STE denote the fully connected layer and the spatio-temporal embedding.

$$\hat{Y} = \{\hat{Y}_1, \hat{Y}_2, \dots, \hat{Y}_{T_p}\} \in \mathbb{R}^{T_p \times N \times F}.$$

$$\{\hat{Y}_1, \hat{Y}_2, \dots, \hat{Y}_{T_p}\} = \mathcal{F}(X_1, X_2, \dots, X_{T_h}; \mathcal{G}). \quad (1)$$

Self-Attention. The self-attention is the mostly used attention mechanism. The key idea behind the mechanism is each element in a sequence learns to gather information from other tokens. The input of self-attention consists of queries, keys, and values of dimension d . Then compute the dot products of the query with all keys, divide each by \sqrt{d} , and apply a *softmax* function to obtain the weights on the values:

$$\text{Attention} = \text{softmax}\left(\frac{QK^T}{\sqrt{d}}\right)V. \quad (2)$$

4 METHODOLOGY

At the beginning, historical inputs are transformed to a high dimension space \mathbb{R}^d through a fully connected layer to enhance the representation power of STformer. As shown in Figure 2, STformer adopts a Transformer-like encoder-decoder architecture. The encoder and decoder consist of L identical layers, and each layer of encoder and decoder contains two and three sub-layers, respectively. Each layer of encoder and decoder firstly utilizes NATSA to remove noise and capture the temporal dependence, then uses GBS3A to extract global spatial information efficiently. Besides, decoder utilizes the encoder-decoder self-attention to absorb the historical spatio-temporal information from encoder outputs. We will describe each component in details. Finally, we use a fully connected layer at the bottom of STformer to transform outputs of decoder to predicted values.

4.1 Noise-Aware Temporal Self-Attention

For the multivariate time series forecasting, it is very important to extract the temporal information from historical. However, because of various accidental factors (e.g. car accidents and thunderstorms) in road networks, there is a lot of noise in traffic time series. The

existence of noise makes the temporal information intricate. Prior models are not aware of the negative impact of noise and hard to get accurate patterns from time series with noise. Therefore, we propose NATSA to adaptively denoise time series and capture the stable temporal dependence by combining DWT and neural networks.

DWT decomposes time series into high-frequency component and low-frequency component through a low-pass filter l and a high-pass filter h with 1-level decomposition:

$$X_l, X_h = \text{DWT}(X, l, h), \quad (3)$$

where $X_l \in \mathbb{R}^{\frac{T}{2} \times N \times d}$ and $X_h \in \mathbb{R}^{\frac{T}{2} \times N \times d}$ are the low-frequency component and the high-frequency component of $X \in \mathbb{R}^{T \times N \times d}$ after decomposing and down-sampling in DWT. Figure 1 shows that the low-frequency component is stable and represents the trend of time series, while the high-frequency component is covered by noise. Therefore, the traditional noise-aware methods [6] usually remove noise by setting the part of the high-frequency component that is lower than threshold to zero.

Different from traditional methods, we use a learnable filter $W^D \in \mathbb{R}^{\frac{T}{2} \times N \times d}$ to multiply the high-frequency component $X_h \in \mathbb{R}^{\frac{T}{2} \times N \times d}$ to adjust the weight of each frequency in X_h . The weight of the noise frequency will be reduced by back-propagation. Then we remove the noise in X_h through a non-linear activation function *ReLU*. Formally:

$$DE(X) = \prod_{n=1}^N (\text{ReLU}(W^D^n \odot X_h^n))_N, \quad (4)$$

where \odot and $\prod(\cdot)_N$ indicate the hadamard product and the concatenate operation along with the spatial dimension N .

Moreover, because of the low-frequency component $X_l \in \mathbb{R}^{\frac{T}{2} \times N \times d}$ is stable. We consider it is easier to capture long-term temporal dependence than high-frequency component X_h . Similar to recent work such as GMAN and ST-GRAT, we choose the self-attention to capture the global temporal dependence in X_l . However, using the vanilla temporal self-attention for pure time series is over-fitting and inefficient. Therefore, we use a random coefficient matrix [24] to replace the coefficient matrix obtained by the multiplication of query and key to reduce complexity. Concretely, a learnable parameter matrix $W^C \in \mathbb{R}^{\frac{T}{2} \times \frac{T}{2}}$ is used as the coefficient matrix to update value. Besides, all sensors share the W^C to avoid over-fitting:

$$TA(X) = \prod_{n=1}^N (W^C X_l^n)_N. \quad (5)$$

At the end of NATSA, we use the high-frequency component after denoising and the low-frequency component after global interaction to perform inverse discrete wavelet transform (IDWT) to reconstruct a more stable and temporal interacted time series, formulated as follows:

$$NATSA(X) = \text{IDWT}(TA(X), DE(X)), \quad (6)$$

where $X \in \mathbb{R}^{T \times N \times d}$ is the input of NATSA.

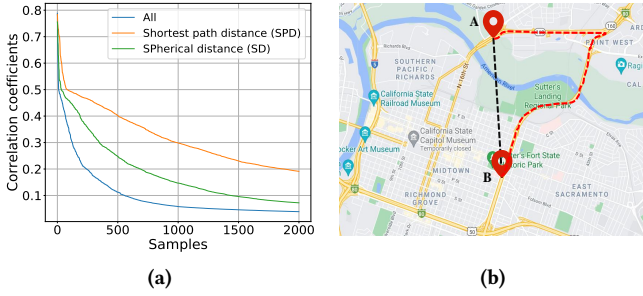


Figure 3: (a): The long-tail distribution of correlation coefficients of spatial self-attention. The orange, green, and blue line denote correlation coefficients of each sensor are sampled from 10 sensors with the shortest path distance, 10 sensors with the shortest spherical distance, and all sensors. (b): The actual shortest path distance (red line) between A and B is larger than the spherical distance (black line).

4.2 Graph-Based Sparse Spatial Self-Attention

Most of the existing efficient Transformer methods use local patterns and lose global information. Informer [36] proves that selecting "active" tokens to be a sparse query to store global information can achieve outstanding performance under the long-tail distribution of coefficient correlations of self-attention. As shown in Figure 3a, the long-tail distribution phenomenon also exists in spatial self-attention. Similar to Informer, we propose the GBS3A to reduce complexity of spatial self-attention by finding most active sensors in the road network and selecting their hidden states from input $X \in \mathbb{R}^{T \times N \times d}$ to be the sparse query $S \in \mathbb{R}^{T \times U \times d}$. The sparse query S can learn global spatial information at all time steps, and U denotes the number of active sensors in the road network. Formulated as:

$$\begin{aligned} GBS3A(X) &= \prod_{t=1}^T (\text{softmax}(\frac{S_t K_t^T}{\sqrt{d}}) V_t)_T \\ S_t &= X_t^{idx_t} W^Q, K_t = X_t W^K, V_t = X_t W^V, \end{aligned} \quad (7)$$

where $\prod(\cdot)_T$ is the concatenate operation along with the temporal dimension T and $W^Q, W^K, W^V \in \mathbb{R}^{d \times d}$ are the learnable parameters of projections. The $idx \in \mathbb{R}^{T \times U}$ indicates the index of selected active sensors. Next we will introduce how to get the idx . Besides, sensors are not selected as the sparse query in GBS3A will be updated with the average of all sensors of the input X in each timestep.

Informer [36] utilizes the ProbSparse Self-Attention (PBSA) to replace the vanilla self-attention, which assumes sensors with correlation coefficients in the query-key coefficients matrix of self-attention away from the uniform distribution are active from the perspective of probability distribution. However, each sensor only samples a few sensors (*w.r.t* only $\log N$ sensors) to calculate the distribution of its correlation coefficients to keep efficiency, it is difficult to reflect the true distribution. Different from PBSA, we sparse the query from the perspective of message passing. We select active sensors that receives max flow from other sensors. To this end, we employ a trainable scalar projection vector $P \in \mathbb{R}^{N \times 1}$ to

project the 2-D coefficient matrix $QK^T \in \mathbb{R}^{N \times N}$ in self-attention to 1-D to evaluate how much flow from other sensors can be retained in query when projected onto the direction of P . Formally:

$$M = \prod_{t=1}^T \left(\frac{(X_t W^Q)(X_t W^K)^T P}{\|P\|} \right)_T, \quad (8)$$

where $M \in \mathbb{R}^{T \times N}$ denotes the activity of each sensor and $\|\cdot\|$ indicates the Frobenius norm.

Then we select U sensors with the largest scalar projection values on the direction of p as the sparse query S and the time complexity of our GBS3A is $O(NU)$. The formula of getting the top- U index from M is:

$$idx = \text{rank}(M, U), \quad (9)$$

where $\text{rank}(\cdot)$ returns the index of the top- U largest values.

Further, the time complexity of eq. 8 is $O(N^2)$. Informer samples a subset of key in all sensors for each sensor to reduce the time complexity of eq. 8. However, as shown in Figure 3a, correlation coefficients of the subset of key which sampled in all sensors (*i.e.* All in Figure 3a) show a more obvious long-tail trend than the subset of key which sampled in sensors with shortest distance (*i.e.* SPD and SD in Figure 3a). Therefore, we argue that the subset of key sampled in all sensors is not enough to reflect the real flow of sensors. Here we select U sensors with the shortest path distance in the road network based graph as a subset of key for each sensor to calculate M , as follows:

$$M = \prod_{t=1}^T \left(\frac{\prod_{n=1}^N ((X_t^n W^Q)(X_t^{idx_k^n} W^K)^T)_N P}{\|P\|} \right)_T, \quad (10)$$

where $p \in \mathbb{R}^{O \times 1}$ and the time complexity of eq. 10 is $O(NO)$. The $idx_k \in \mathbb{R}^{N \times O}$ denotes the index of the subset of key for each sensor. As for the choice of the shortest path distance, because of the spherical distance may be misleading, e.g., the spherical distance between sensor A and sensor B is close but the actual distance between them in the road network is very far in Figure 3b.

Finally, we analyze why choose the sparse query instead of the sparse key to optimize self-attention. The spatial receptive field of the sparse key is limited. Even if the sampled subset of key contains most of the information, a small part is missing. We choose sparse query to optimize vanilla self-attention because the use of the sparse query ensures we can get the global spatial information through active sensors.

4.3 Other Components

4.3.1 Encoder-Decoder Self-Attention. Similar to the vanilla Transformer, we use the Encoder-Decoder Self-Attention (EDA) at the end of each layer of the decoder to extract historical spatio-temporal information, formulated as:

$$\begin{aligned} EDA(X_{en}, X_{de}) &= \prod_{n=1}^N \left(\text{softmax} \left(\frac{Q^n K^{nT}}{\sqrt{d}} \right) V^n \right)_N \\ Q^n &= X_{de}^n W^Q, K^n = X_{en}^n W^K, V^n = X_{en}^n W^V, \end{aligned} \quad (11)$$

where $X_{en} \in \mathbb{R}^{T_h \times N \times d}$ and $X_{de} \in \mathbb{R}^{T_p \times N \times d}$ denote the output of encoder and the output of previous layer of EDA.

Specifically, at the top of the decoder, we use the future spatio-temporal embedding and the historical spatio-temporal embedding

as the query and key in EDA to perform generative style inference instead of step-by-step decoding, which reduces the cumulative error and time consumption of long-term prediction. We put the details of spatio-temporal embedding (STE) in Appendix A.

Multi-Head Mechanism. At present, researchers use multi-head self-attention to get more information from different sub-spaces, and all the self-attention operations in our STformer adopt the multi-head mechanism, as shown below:

$$\text{MultiHead}(X) = W^H \prod_{h=1}^H (\text{head}_h)_H \quad (12)$$

where $\text{head}_h = \text{Attention}(X)$,

where H denotes the number of head, $\prod(\cdot)_H$ is a concatenate operation along with feature dimension H . Each head has three linear projections to project the input to query, key and value. The W_h^Q , W_h^K , $W_h^V \in \mathbb{R}^{d \times \frac{d}{H}}$ are learnable parameters of linear projections in each head and $W^H \in \mathbb{R}^{d \times d}$ is the learnable parameter of output projection.

4.4 Loss Function.

STformer can be trained end-to-end via back-propagation by minimizing the L1 Loss between the predicted values and ground truths:

$$\mathcal{L}(\Theta) = \sum_{t=1}^{T_p} \sum_{i=1}^N |Y_t^i - \hat{Y}_t^i|, \quad (13)$$

where Θ denotes all learnable parameters in STformer.

4.5 Complexity Analysis

In the following analysis we compute the complexity involved in a single layer of the encoder and the decoder with T timesteps. The complexity of GBS3A is $O(TN \log N)$ because of $U \approx \log N$ and $O \approx \log N$. NATSA has dominant complexity $O(\frac{1}{4}NT^2d)$, as is evident from eq. (4) and eq. (5). Besides, the complexity of EDA follows the vanilla temporal self-attention and is $O(NT^2d)$. Therefore, the complexity of the single layer in encoder and decoder is $O(TN(\frac{T}{4} + \log N)d)$ and $O(TN(\frac{5T}{4} + \log N)d)$.

5 EXPERIMENTS

5.1 Datasets

We use four large-scale datasets in traffic forecasting to evaluate the performance of our model, which are PEMSD3, PEMSD4, PEMSD7, and PEMSD8 [23]. They are all collected by California Transportation Agencies (CalTrans) Performance Measurement System (PeMS) [4]. The detailed information is shown in Table 1.

Data Preprocessing. We split these four datasets into a training set (60%), validation set (20%), and test set (20%) in chronological order following the previous work [23]. In order to meet the traffic prediction requests of users in the real world, we use historical traffic data for three hours (*i.e.* 36 timesteps) to predict next three hours traffic volume. We further utilize the z-score normalization to normalize the input data and re-normalize the output of model to make our model more stable. Besides, we use a pre-defined graph which based on the actual road network as prior knowledge. More

Dataset	#Nodes	#Edges	#Samples	Sample Rate	#MissingRatio
PEMSD3	358	547	26208	5 mins	0.672%
PEMSD4	307	340	16992	5 mins	3.182%
PEMSD7	883	866	28224	5 mins	0.452%
PEMSD8	170	295	17856	5 mins	0.696%

Table 1: Dataset statistics

details about z-score normalization can be found in the Appendix B.

5.2 Experimental Settings

Baselines. We compare STformer with widely used baselines and state-of-the-art models to evaluate the overall performance of our work, including 1) DCRNN [14]: a diffusion convolutional recurrent neural network, which utilizes the diffusion convolution in GRU to extract spatial information; 2) STGCN [34]: a spatial-temporal graph convolutional network, which combines GCN with GLU to capture spatio-temporal dependencies; 3) STGCN [23]: a spatial-temporal synchronous graph convolutional network, which designs the spatial-temporal synchronous modeling mechanism; 4) STFGNN [18]: an advanced version of STGCN, which uses FastDTW to create the temporal graph; 5) Ggraph WaveNet [33]: a spatial-temporal graph convolutional network, which combines the self-adaptive adjacency matrix based GCN with TCN; 6) AGCRN [2]: an adaptive graph convolutional recurrent network, which integrates the GRU with the self-adaptive adjacency matrix based GCN; 7) GMAN [35]: a variant of the Transformer network that uses the self-attention mechanism for temporal and spatial dimensions; 8) ST-GRAT [19]: a variant of the Transformer network that takes the external graph structure information (*e.g.* distance between roads) in spatial self-attention. The details of baselines in Appendix C.

Metrics. We use the Mean Absolute Errors (MAE), Mean Absolute Percentage Errors (MAPE), and Root Mean Squared Errors (RMSE) to measure the performance of models. The detailed information of evaluation metrics MAE, RMSE, and MAPE in Appendix D.

Experimental Environment. All models are implemented in Pytorch 1.7.1 and executed on a server with the Tesla V100S-PCIe 32GB GPU. We repeat all experiments 5 times and report the average of evaluation metrics.

Parameter Settings. In STformer, we set the layer $L = 3$, the feature size $d = 128$, and the head number $H = 8$ according to the previous work [19]. The batchsize is 16 except 8 on the PEMSD7 dataset. Besides, we adopt the Adam [10] optimizer with the initial learning rate of 0.001 in STformer. The optimal setting of O and U are $\log N$ according to the Appendix E.

5.3 Main Results

Due to space limit, Table 2 summarizes prediction performances of two larger datasets PEMSD3 and PEMSD7, which are the MAE, RMSE, and MAPE over next one, two, and three hours of our

Dataset	Method	1 Hour			2 Hour			3 Hour		
		MAE	RMSE	MAPE (%)	MAE	RMSE	MAPE (%)	MAE	RMSE	MAPE (%)
PEMSD3	DCRNN	18.97	32.99	18.34	23.35	41.19	21.59	27.21	46.99	25.58
	STGCN	18.75	32.79	17.82	23.55	40.31	21.58	28.25	47.72	25.59
	STSGCN	19.60	32.69	18.49	23.71	39.65	22.42	27.42	47.04	22.59
	STFGNN	18.57	31.19	17.15	21.74	36.42	20.23	24.60	41.55	23.15
	Graph WaveNet	17.20	30.71	16.93	19.57	34.26	19.36	21.77	35.47	20.73
	AGCRN	17.90	30.52	17.02	19.29	34.10	19.28	21.72	35.87	20.86
	GMAN	18.04	31.22	17.84	18.99	33.56	19.19	20.22	34.47	19.95
	ST-GRAT	<u>16.94</u>	<u>30.24</u>	<u>16.84</u>	<u>18.91</u>	<u>33.98</u>	<u>18.95</u>	23.61	37.60	21.68
	STformer (ours)	16.07	28.77	16.18	17.82	31.03	17.81	19.29	32.87	19.16
PEMSD7	Improvement	+5.14%	+4.86%	+3.92%	+5.76%	+7.54%	+6.02%	+4.60%	+4.64%	+3.96%
	DCRNN	30.00	45.11	14.02	35.95	53.00	16.44	39.13	58.09	16.74
	STGCN	29.22	44.52	12.40	37.01	54.19	15.45	43.50	62.76	17.59
	STSGCN	26.56	44.27	11.19	32.27	55.43	13.86	36.55	59.54	16.17
	STFGNN	25.13	43.15	10.94	30.50	53.06	13.03	31.67	55.60	13.79
	Graph WaveNet	<u>22.41</u>	<u>38.66</u>	<u>9.57</u>	<u>24.72</u>	<u>41.25</u>	10.70	<u>27.02</u>	45.46	12.03
	AGCRN	23.08	<u>38.02</u>	9.83	24.92	41.79	<u>10.63</u>	27.21	<u>45.24</u>	<u>11.77</u>
	GMAN	OOM			ST-GRAT	OOM				
	STformer (ours)	20.79	36.02	8.68	22.22	38.89	9.37	23.40	40.96	10.01
	Improvement	+7.23%	+5.26%	+9.30%	+10.11%	+5.72%	+11.85%	+13.40%	+9.46%	+14.95%

Table 2: Performance comparison of STformer and baselines on PEMSD3 and PEMSD7. The bold font and underline indicates the optimal and sub-optimal performances, respectively. The Improvement denotes the reduction of the optimal results compared with the sub-optimal result. Besides, GMAN and ST-GRAT ran out of GPU memory (OOM) on the PEMSD7 dataset.

Variant	MAE	RMSE	MAPE	Improvement
Basic	18.70	32.32	19.07	-
+ NATSA	17.91	31.86	18.50	+4.22%
+ GBS3A (ours)	16.87	29.83	16.97	+9.79%

Table 3: Results for ablation study on the PEMSD3 dataset. The Improvement denotes the reduction of MAE.

Variant	Memory Usage	MAE	RMSE	MAPE	Improvement
Temporal View					
VTSA	34818 M	17.47	30.35	18.92	-
NAVTSA	28541 M	17.38	30.25	18.63	+0.52%
NATSA (ours)	24701 M	16.87	29.83	16.97	+3.43%
Spatial View					
VSSA	56814 M	17.85	31.27	17.52	-
PBSA (Informer)	25749 M	17.43	31.21	17.26	+2.35%
GBS3A-SD	24701 M	17.14	30.57	17.06	+3.98%
GBS3A (ours)	24701 M	16.87	29.83	16.97	+5.49%

Table 4: Comparison of different self-attention methods on the temporal view and spatial view. The Improvement denotes the reduction of MAE.

STformer and eight representative comparison methods. The results of the other two datasets PEMSD4 and PEMSD8 are shown in Appendix F.

We draw the following conclusions from the experimental results: 1) STGCN and DCRNN first combine graph convolutional network (GCN) with deep time series models (e.g. RNN and 1D-CNN) to extract spatio-temporal dependencies, their performance are improved compared with traditional methods. 2) Based on the above two models, Graph WaveNet and AGCRN use the self-adaptive adjacency matrix based GCN and achieve better results than the road network based DCRNN and STGCN. 3) STSGCN and STFGNN design the spatio-temporal synchronous mechanism and the spatio-temporal fusion graph to increase receptive field of GCN to improve performance, respectively. 4) GMAN and ST-GRAT are the Transformer-like models, they apply vanilla self-attention to two dimensions of temporal and spatial in traffic forecasting tasks and achieve better results than GCN-based methods because of the global receptive field of self-attention. However, the existing Transformer-based models are limited by the quadratic issue and difficult to handle large-scale datasets.

STformer adopts a Transformer-like architecture, which uses not only GBS3A to efficiently extract global spatial information, but also combines DWT with neural networks to propose NATSA to adaptively denoise the input and hidden states. Therefore, it is natural that STformer shows much better performances against above baselines and improves a maximum of 13.4% on MAE, 9.46% on RMSE, and 14.95% on MAPE. Besides, results of STformer on PEMSD7 is better than the simple dataset PEMSD3.

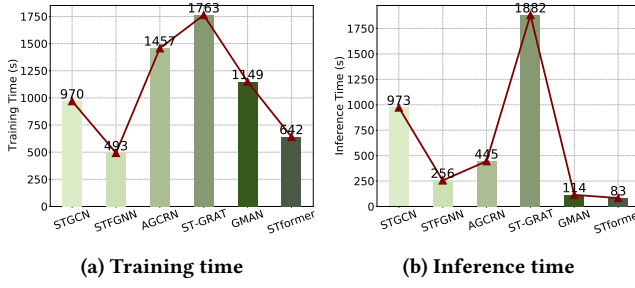


Figure 4: The computation time on the PEMSD3 dataset.

5.4 Ablation Study

To verify the effectiveness of NATSA and GBS3A in STformer, we sequentially add NATSA (*i.e.* + NATSA in Table 3) and GBS3A (*i.e.* + GBS3A in Table 3) on the Basic to capture spatio-temporal dependencies. The Basic model includes the EDSA layer, the Feed-Forward and the residual connection. As shown in Table 3, NATSA and GBS3A improve the prediction accuracy of STformer.

5.5 Spatio-Temporal Study

Temporal Study. To further estimate the effect of NATSA, we replace NATSA with the vanilla temporal self-attention (*i.e.* VTSA in Table 4) and the noise-aware vanilla temporal self-attention (*i.e.* NAVTSA in Table 4). By comparing results of VTSA and NAVTSA, we found that removing noise and extracting temporal patterns on the high and low-frequency component of time series after DWT can reduce the memory usage and improve model performance. We further found that using VTSA on the low-frequency component does not significantly improve the prediction accuracy. We speculate that the pure time series does not require a complicated deep time series model. Therefore, STformer utilizes the random coefficient matrix shared by sensors and improves the forecasting performance.

Spatial Study. To further estimate the effect of GBS3A, we replace GBS3A with the vanilla spatial self-attention (*i.e.* VSSA in Table 4), the ProbSparse Self-Attention in Informer (*i.e.* PBSA in Table 4), and GBS3A with the subset of key based on the spherical distance (*i.e.* GBS3A-SD in Table 4). As shown in Table 4, methods use sparse query reduce the memory usage and improve the performance of STformer compared with VSSA, because of the full self-attention is low-rank and has useless information. Besides, our graph-based sparse methods avoids to get the wrong distribution of correlation coefficients compared with PBSA and further improves the prediction accuracy. Moreover, the shortest path distance can better reflect spatial correlations between sensors than directly using the spherical distance.

5.6 Computation Cost

As shown in Figure 4, STformer reduces the training and inference time compared with other Transformer-based models. Moreover, the inference time of ST-GRAT and STGCN that utilizes step-by-step dynamic decoding is higher than other generative models in Figure 4b. Besides, using RNN will increase the training and

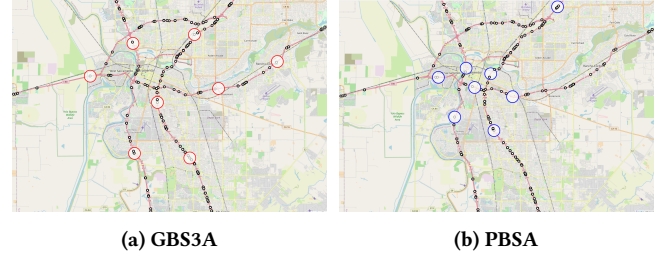


Figure 5: Visualization of sensors in the PEMSD3. Red and blue circles in (a) and (b) are the learnt sparse query of GBS3A and PBSA that appears most frequently in all heads.

inference time consumption, such as AGCRN, because RNN cannot be paralleled.

5.7 Visualization

Figure 5 visualizes the learnt sparse query of using GBS3A and PBSA in STformer on the PEMSD3 dataset. We found that active sensors in the sparse query obtained by GBS3A and PBSA are distributed on different road segments, so that different active sensors will extract global and diverse spatial information that is more focused on their distributed road segments. The difference of them is that active sensors obtained by GBS3A are distributed in the middle of the road segment and active sensors obtained by PBSA are distributed at the ends of the road segment. When the active sensor at one end of the road segment, it is easy to ignore information at the other end, resulting in lower performance.

6 CONCLUSION

In this paper, we propose a novel noise-aware efficient Transformer architecture for traffic forecasting, named STformer. STformer uses NATSA to capture more stable temporal properties in denoised time series and uses GBS3A to capture the global spatial dependence more efficiently. Extensive experiments on multi-step traffic forecasting tasks demonstrate the effectiveness of both STformer and the proposed modules. In the future, we will look for applying STformer to other multivariate time-series forecasting applications, such as travel demand, stock price prediction, and electricity used forecasting.

REFERENCES

- [1] Dzmitry Bahdanau, Kyunghyun Cho, and Yoshua Bengio. 2014. Neural machine translation by jointly learning to align and translate. *arXiv preprint arXiv:1409.0473* (2014).
- [2] Lei Bai, Lina Yao, Can Li, Xianzhi Wang, and Can Wang. 2020. Adaptive Graph Convolutional Recurrent Network for Traffic Forecasting. In *Advances in Neural Information Processing Systems 33: Annual Conference on Neural Information Processing Systems, virtual*.
- [3] Iz Beltagy, Matthew E Peters, and Arman Cohan. 2020. Longformer: The long-document transformer. *arXiv preprint arXiv:2004.05150* (2020).
- [4] Chao Chen, Karl Petty, Alexander Skabardonis, Pravin Varaiya, and Zhanfeng Jia. 2001. Freeway performance measurement system: mining loop detector data. *Transportation Research Record* 1748, 1 (2001), 96–102.
- [5] Rewon Child, Scott Gray, Alec Radford, and Ilya Sutskever. 2019. Generating long sequences with sparse transformers. *arXiv preprint arXiv:1904.10509* (2019).
- [6] David L Donoho and Jain M Johnstone. 1994. Ideal spatial adaptation by wavelet shrinkage. *biometrika* 81, 3 (1994), 425–455.
- [7] David A Forsyth and Jean Ponce. 2012. *Computer vision: a modern approach*. Pearson..

[8] Ian Goodfellow, Yoshua Bengio, Aaron Courville, and Yoshua Bengio. 2016. *Deep learning*. Vol. 1. MIT press Cambridge.

[9] Frederick Jelinek. 1997. *Statistical methods for speech recognition*. MIT press.

[10] Diederik P. Kingma and Jimmy Ba. 2015. Adam: A Method for Stochastic Optimization. In *3rd International Conference on Learning Representations, ICLR 2015, San Diego, CA, USA, May 7-9, 2015, Conference Track Proceedings*.

[11] Nikita Kitaev, Lukasz Kaiser, and Anselm Levskaya. 2020. Reformer: The Efficient Transformer. In *8th International Conference on Learning Representations, ICLR 2020, Addis Ababa, Ethiopia, April 26-30, 2020*.

[12] Colin Lea, Michael D Flynn, Rene Vidal, Austin Reiter, and Gregory D Hager. 2017. Temporal convolutional networks for action segmentation and detection. In *proceedings of the IEEE Conference on Computer Vision and Pattern Recognition*. 156–165.

[13] Juho Lee, Yoonho Lee, Jungtaek Kim, Adam Kosiorek, Seungjin Choi, and Yee Whye Teh. 2019. Set transformer: A framework for attention-based permutation-invariant neural networks. In *International Conference on Machine Learning*. PMLR, 3744–3753.

[14] Yaguang Li, Rose Yu, Cyrus Shahabi, and Yan Liu. 2018. Diffusion Convolutional Recurrent Neural Network: Data-Driven Traffic Forecasting. In *6th International Conference on Learning Representations, ICLR 2018, Vancouver, BC, Canada, April 30 - May 3, 2018, Conference Track Proceedings*.

[15] Elizabeth D Liddy. 2001. Natural language processing. (2001).

[16] Zheng Lu, Chen Zhou, Jing Wu, Hao Jiang, and Songyue Cui. 2016. Integrating granger causality and vector auto-regression for traffic prediction of large-scale WLANs. *KSII Transactions on Internet and Information Systems (TIIIS)* 10, 1 (2016), 136–151.

[17] Thang Luong, Hieu Pham, and Christopher D. Manning. 2015. Effective Approaches to Attention-based Neural Machine Translation. In *Proceedings of the 2015 Conference on Empirical Methods in Natural Language Processing, EMNLP 2015, Lisbon, Portugal, September 17-21, 2015*. 1412–1421.

[18] Li Mengzhang and Zhu Zhanxing. 2020. Spatial-Temporal Fusion Graph Neural Networks for Traffic Flow Forecasting. *arXiv preprint arXiv:2012.09641* (2020).

[19] Cheonbok Park, Chunggi Lee, Hyojin Bahng, Yunwon Tae, Seungmin Jin, Kihwan Kim, Sungahn Ko, and Jaegul Choo. 2020. ST-GRAT: A Novel Spatio-temporal Graph Attention Networks for Accurately Forecasting Dynamically Changing Road Speed. In *Proceedings of the 29th ACM International Conference on Information & Knowledge Management*. 1215–1224.

[20] Niki Parmar, Ashish Vaswani, Jakob Uszkoreit, Lukasz Kaiser, Noam Shazeer, Alexander Ku, and Dustin Tran. 2018. Image transformer. In *International Conference on Machine Learning*. PMLR, 4055–4064.

[21] Auroko Roy, Mohammad Saffar, Ashish Vaswani, and David Grangier. 2021. Efficient content-based sparse attention with routing transformers. *Transactions of the Association for Computational Linguistics* 9 (2021), 53–68.

[22] Mark J Shensa et al. 1992. The discrete wavelet transform: wedding the a trous and Mallat algorithms. *IEEE Transactions on signal processing* 40, 10 (1992), 2464–2482.

[23] Chao Song, Youfang Lin, Shengnan Guo, and Huaiyu Wan. 2020. Spatial-temporal synchronous graph convolutional networks: A new framework for spatial-temporal network data forecasting. In *Proceedings of the AAAI Conference on Artificial Intelligence*, Vol. 34. 914–921.

[24] Yi Tay, Dara Bahri, Donald Metzler, Da-Cheng Juan, Zhe Zhao, and Che Zheng. 2021. Synthesizer: Rethinking self-attention for transformer models. In *International Conference on Machine Learning*. PMLR, 10183–10192.

[25] JWC Van Linh and CPIJ Van Hinsbergen. 2012. Short-term traffic and travel time prediction models. *Artificial Intelligence Applications to Critical Transportation Issues* 22, 1 (2012), 22–41.

[26] Ashish Vaswani, Noam Shazeer, Niki Parmar, Jakob Uszkoreit, Llion Jones, Aidan N. Gomez, Łukasz Kaiser, and Illia Polosukhin. 2017. Attention is All you Need. In *Advances in Neural Information Processing Systems 30: Annual Conference on Neural Information Processing Systems 2017, December 4-9, 2017, Long Beach, CA, USA*. 5998–6008.

[27] Xiaoyang Wang, Yao Ma, Yiqi Wang, Wei Jin, Xin Wang, Jiliang Tang, Caiyan Jia, and Jian Yu. 2020. Traffic flow prediction via spatial temporal graph neural network. In *Proceedings of The Web Conference 2020*. 1082–1092.

[28] Yunbo Wang, Zhifeng Gao, Mingsheng Long, Jianmin Wang, and S Yu Philip. 2018. Predrnn++: Towards a resolution of the deep-in-time dilemma in spatiotemporal predictive learning. In *International Conference on Machine Learning*. PMLR, 5123–5132.

[29] Yunbo Wang, Mingsheng Long, Jianmin Wang, Zhifeng Gao, and Philip S Yu. 2017. Predrnn: Recurrent neural networks for predictive learning using spatiotemporal lstms. In *Proceedings of the 31st International Conference on Neural Information Processing Systems*. 879–888.

[30] Billy M Williams and Lester A Hoel. 2003. Modeling and forecasting vehicular traffic flow as a seasonal ARIMA process: Theoretical basis and empirical results. *Journal of transportation engineering* 129, 6 (2003), 664–672.

[31] Chun-Hsin Wu, Jan-Ming Ho, and Der-Tsai Lee. 2004. Travel-time prediction with support vector regression. *IEEE transactions on intelligent transportation systems* 5, 4 (2004), 276–281.

[32] Lin Wu, Michele Haynes, Andrew Smith, Tong Chen, and Xue Li. 2017. Generating Life Course Trajectory Sequences with Recurrent Neural Networks and Application to Early Detection of Social Disadvantage. In *Advanced Data Mining and Applications - 13th International Conference, ADMA 2017, Singapore, November 5-6, 2017, Proceedings*, Vol. 10604. 225–242.

[33] Zonghan Wu, Shirui Pan, Guodong Long, Jing Jiang, and Chengqi Zhang. 2019. Graph WaveNet for Deep Spatial-Temporal Graph Modeling. In *Proceedings of the Twenty-Eighth International Joint Conference on Artificial Intelligence, IJCAI 2019, Macao, China, August 10-16, 2019*. 1907–1913.

[34] Bing Yu, Haoteng Yin, and Zhanxing Zhu. 2018. Spatio-Temporal Graph Convolutional Networks: A Deep Learning Framework for Traffic Forecasting. In *Proceedings of the Twenty-Seventh International Joint Conference on Artificial Intelligence, IJCAI 2018, July 13-19, 2018, Stockholm, Sweden*. 3634–3640.

[35] Chuanpan Zheng, Xiaoliang Fan, Cheng Wang, and Jianzhong Qi. 2020. Gman: A graph multi-attention network for traffic prediction. In *Proceedings of the AAAI Conference on Artificial Intelligence*, Vol. 34. 1234–1241.

[36] Haoyi Zhou, Shanghang Zhang, Jieqi Peng, Shuai Zhang, Jianxin Li, Hui Xiong, and Wancai Zhang. 2020. Informer: Beyond Efficient Transformer for Long Sequence Time-Series Forecasting. *arXiv preprint arXiv:2012.07436* (2020).